Continuous evolution of functions and measures toward fixed points of contraction mappings

Jerry L. Bona[1] and Edward R. Vrscay[2]

[1] Department of Mathematics, Statistics and Computer Science
The University of Illinois at Chicago
Chicago, Illinois, USA 60607-7045
bona@math.uic.edu

[2] Department of Applied Mathematics
University of Waterloo
Waterloo, Ontario, Canada N2L 3G1
ervrscay@uwaterloo.ca

Summary. Let T be a contraction mapping on an appropriate Banach space $B(X)$. Then the evolution equation $y_t = Ty - y$ can be used to produce a continuous evolution $y(x,t)$ from an arbitrary initial condition $y_0 \in B(X)$ to the fixed point $\bar{y} \in B(X)$ of T. This simple observation is applied in the context of iterated function systems (IFS). In particular, we consider (1) the Markov operator M (on a space of probability measures) associated with an N-map IFS with probabilities (IFSP) and (2) the fractal transform T (on functions in $L^1(X)$, for example) associated with an N-map IFS with greyscale maps (IFSM), which is generally used to perform fractal image coding. In all cases, the evolution equation takes the form of a nonlocal differential equation.

Such an evolution equation technique can also be applied to complex analytic mappings which are not strictly contractive but which possess invariant attractor sets. A few simple cases are discussed, including Newton's method in the complex plane.

1 Introduction

In this paper we introduce a class of evolution equations associated with contraction mappings on a Banach space of functions $B(X)$. The purpose is to produce a *continuous evolution* toward the fixed point $\bar{x}$ of a contraction map T, as opposed to the usual discrete sequence of iterates $x_n = T^n x_0$ that converge to $\bar{x}$.

The original motivation to devise such evolution equations arose from a desire to perform continuous, yet fractal-like, (i.e., spatially-contracted and greyscale distorted) "touch-up" operations on images. A fractal-based evolution method could be used to produce arbitarily small local alterations to an image $u(x)$ in a neigh-

bourhood of a point $x_0 \in X$ that depend upon the behaviour of u at other regions of X.

In addition to applying the idea to contractive fractal transform operators, we show briefly that such methods can also be applied to to other mappings, e.g., complex analytic mappings, that possess invariant attractor sets. While a few simple cases are examined here, a more thorough investigation will be reported in a future paper.

The structure of this paper is as follows. In Section 2, we introduce the class of evolution equations which take the form of differential equations involving functions or measures on an appropriate complete metric space (X, d). Section 3 reviews the basics of N-map Iterated Function Systems with probabilities (IFSP) and associated invariant measures. In Section 4 is constructed an evolution equation scheme so that time-dependent probability measures will evolve continuously (in time) to the invariant measure $\bar{\mu}$ of an IFSP. In Section 5, we consider IFS-type fractal transform operators on functions and illustrate the evolution scheme on a fractally-coded image. In Section 6, some simple applications of the evolution method to complex analytic dynamics are briefly considered, namely (i) iteration of quadratic maps and (ii) Newton's method in the complex plane.

2 Evolution equations associated with contractive mappings on Banach spaces

In all that follows, X will denote a closed and bounded subset of $\mathbf{R}^n$, $n = 1, 2, \cdots$, with d the Euclidean metric on X. Let $B(X)$ denote a Banach space of functions defined on X. Suppose that $T : B(X) \to B(X)$ is a contraction mapping, which is to say

$$\| Tu - Tv \| \leq c_T \| u - v \|, \quad \text{for all } u, v \in B(X), \tag{1}$$

where $c_T \in [0, 1)$. From Banach's fixed point theorem, there exists a unique $\bar{y} \in B(X)$ such that $\bar{y} = T\bar{y}$. Moreover, if, for any $y_0 \in B(X)$, we define the iteration sequence $y_{n+1} = Ty_n$, $n = 0, 1, \cdots$, then $\| y_n - \bar{y} \| \to 0$ as $n \to \infty$.

The goal is to produce a continuous evolution from the initial condition y_0 to the fixed point $\bar{y}$. In other words, from the initial condition y_0, we aim to find a function $y(t)$ that converges to $\bar{y}$ as $t \to \infty$, i.e., $\| y(t) - \bar{y} \| \to 0$ as $t \to \infty$. Consider the evolution equation

$$\frac{\partial y}{\partial t} = Ty - y, \tag{2}$$

where $y = y(x, t)$, $x \in X$, $t \geq 0$. Clearly the fixed point function $\bar{y}$ is a solution of this equation – an *equilibrium solution* in the parlance of dynamical systems theory. One immediately wants to know whether this equilibrium solution is globally asymptotically stable, i.e, whether all solutions $y(t)$ to Eq. (2) converge to $\bar{y}$.

Example: Let $Ty = \frac{1}{2}y + \frac{1}{2}$ for $y \in L^1([0, 1])$, say. Then $\bar{y}(x) \equiv 1$ is the unique fixed point of T. In this simple case, where T does not involve any operations on x, the evolution of y is rather simple. For a given $y(x, 0)$, the unique solution to Eq. (2) is

$$y(x, t) = [y(x, 0) - 1]e^{-t/2} + 1, \tag{3}$$

and we see that $y(x, t) \to \bar{y}(x)$ for all $x \in [0, 1]$.

Theorem 1. *Let $B(X)$ be a real Banach space and $T : B(X) \to B(X)$ a contraction map on $B(X)$ with fixed point function $\bar{y}$. Then for any initial value $y(x,0) = y_0(x) \in B(X)$, the solution $y(t)$ converges exponentially rapidly to $\bar{y}$ as $t \to \infty$.*

Remark 1. By a solution of Eq. (2), we mean a C^1-curve $y : [0,\infty) \to B(X)$ such that (2) is satisfied for each $t > 0$.

Proof. First, rewrite Eq. (2) as

$$\frac{\partial y}{\partial t} + y = Ty. \tag{4}$$

Duhamel's formula leads in the usual way to the equation

$$y(t) = y_0 e^{-t} + e^{-t} \int_0^t e^s (Ty)(s) ds. \tag{5}$$

In the special case $y_0 = \bar{y}$, we have $y(t) = \bar{y} = T\bar{y}$ and

$$\bar{y} = \bar{y} e^{-t} + e^{-t} \int_0^t e^s (T\bar{y})(s) ds. \tag{6}$$

Subtracting (6) from (5), one obtains

$$y(t) - \bar{y} = \big(y_0 - \bar{y}\big) e^{-t} + e^{-t} \int_0^t e^s \big(Ty(s) - T\bar{y}\big) ds. \tag{7}$$

By Minkowski's integral inequality, it follows that

$$\| y(t) - \bar{y} \| \leq \| y_0 - \bar{y} \| e^{-t} + e^{-t} \int_0^t e^s \| Ty(s) - T\bar{y} \| ds, \tag{8}$$

where the norm is that of $B(X)$. Contractivity of T gives

$$\| y(t) - \bar{y} \| \leq \| y_0 - \bar{y} \| e^{-t} + c_T e^{-t} \int_0^t e^s \| y(s) - \bar{y} \| ds, \tag{9}$$

Gronwall's lemma then implies that for $t > 0$,

$$\| y(t) - \bar{y} \| \leq \| y_0 - \bar{y} \| e^{(c_T - 1)t}. \tag{10}$$

Since $0 \leq c_T < 1$, it follows that $\| y(t) - \bar{y} \| \to 0$ as $t \to \infty$ and exponentially rapidly, in fact, and the theorem is proved.

2.1 Practicalities and the discretization of the evolution equation

Attention is now turned to a few practicalities of solving the evolution equation in (2). In the computations reported below, we have employed a very simple forward Euler scheme to compute $y(t)$. If $h > 0$ denotes the time step and y_0 the initial condition, then letting $y_n = y(nh)$, for $n = 1, 2, \cdots$, we have

$$y_{n+1} = y_n + (Ty_n - y_n)h, \quad n = 0, 1, 2, \cdots. \tag{11}$$

Note that for $h = 1$, the above scheme reduces to the usual iteration procedure $y_{n+1} = Ty_n$. In fact, the above recursion relation may be rewritten as

$$\begin{aligned} y_{n+1} &= Uy_n \\ &= hTy_n + (1-h)y_n, \quad n = 0, 1, 2, \cdots, \end{aligned} \tag{12}$$

which is a linear interpolation between y_n and Ty_n. If T is a contraction with Lipschitz factor $c_T \in [0, 1)$, then U has Lipschitz factor $c_U = 1 - h(1 - c_T)$. If $0 < h \leq 1$, then U is a contraction and the fixed point of U is $\bar{y}$, the fixed point of T. In Section 3, we shall apply this method to contractive fractal transforms (Iterated Function Systems with greyscale maps) on $L^1(X)$.

Note that the repeated application of the Euler operator U can be written as

$$U^n = \sum_{k=1}^{n} \binom{n}{k} (1-h)^{n-k} \, h^k \, T^k. \tag{13}$$

This can have some interesting consequences on the evolution of $y(t)$ to the fixed point $\bar{y}$ of T. For example, suppose that $h = 1/N$ where $N > 1$. Then the Euler scheme over a fixed time interval, say between $t = 0$ and $t = 1$, will involve higher iterations of the operator T than the simple discrete iteration process $y_1 = Ty_0$ corresponding to $h = 1$. In the same way, a higher-order scheme for the integration of the evolution equation (2) will also yield a more subtle approximation than does straightforward iteration.

Suppose that the starting function y_0 is "flat," for example, a constant function on X. Then in the case that T is a fractal transform operator which produces spatial contractions of a function (see Section 5), the resulting function $U^N y_0$ could have much more spatial detail than the iterate $u_1 = Tu_0$, although the higher-frequency components will probably have rather low amplitude. This clearly indicates that the C^1-curve $y(t)$ does not have to pass through, i.e., interpolate, the discrete sequence $y_n = T^n y_0$, $n \geq 0$. The prospect for enhanced spatial detail may become even more pronounced when higher order integration schemes, e.g., Runge Kutta methods, are used to approximate the differential equation. The points that arise from such considerations are currently being investigated.

In the next section, we introduce Iterated Function Systems in their original setting, namely, applied to probability measures on a compact set X.

3 Iterated Function Systems and invariant imeasures

The idea of defining an operator through the parallel action of a set of contraction maps can be traced back to a number of papers, for example, [16]. However, the use of such systems of maps to construct fractal sets and supporting measures was described independently by Hutchinson [11] and Barnsley and Demko [2]. The latter paper introduced the appelation "Iterated Function Systems".

In what follows, (X, d) denotes a compact metric "base space," typically $[0, 1]^n$. Let $\mathbf{w} = \{w_1, \cdots, w_N\}$ be a set of contraction maps $w_i : X \to X$, to be referred to as an N-map IFS. Let $c_i \in [0, 1)$ denote the contraction factors of the w_i and define $c = \max_{1 \leq i \leq N} c_i$. Note that $c \in [0, 1)$.

Now let $\mathcal{H}(X)$ denote the set of nonempty compact subsets of X and h the Hausdorff metric. Then $(\mathcal{H}, h)$ is a complete metric space [7]. Associated with the IFS maps w_i is a set-valued mapping $\hat{\mathbf{w}} : \mathcal{H}(X) \to \mathcal{H}(X)$ the action of which is defined to be

$$\hat{\mathbf{w}}(S) = \bigcup_{i=1}^{N} w_i(S), \qquad S \in \mathcal{H}(X), \tag{14}$$

where $w_i(S) := \{w_i(x), x \in S\}$ is the image of S under w_i, $i = 1, 2, \cdots, N$.

It is a standard result that $\hat{\mathbf{w}}$ is a contraction mapping on $(\mathcal{H}(X), h)$ [11]; in fact,

$$h(\mathbf{w}(A), \mathbf{w}(B)) \leq ch(A, B), \quad A, B \in \mathcal{H}(X). \tag{15}$$

Consequently, there exists a unique set $A \in \mathcal{H}(X)$, such that $\mathbf{w}(A) = A$, the so-called *attractor* of the IFS $\mathbf{w}$. Moreover, for any $S_0 \in \mathcal{H}(X)$, the sequence of sets $S_n \in \mathcal{H}(X)$ defined by $S_{n+1} = \hat{\mathbf{w}}(S_n)$ converges in Hausdorff metric to A.

Examples:

1. $X = [0, 1]$, $N = 2$: $w_1(x) = \frac{1}{3}x$, $w_2(x) = \frac{1}{3}x + \frac{2}{3}$. Then the attractor A is the ternary Cantor set C on $[0, 1]$.
2. $X = [0, 1]$, $N = 2$: $w_1(x) = sx$, $w_2(x) = sx + (1 - s)$ for $0 < s < 1$. Then $A = [0, 1]$. If $s = 0$ then $A = \{0, 1\}$.

Let $\mathcal{M}(X)$ denote the set of Borel probability measures on X and d_M the Monge-Kantorovich metric on this set:

$$d_M(\mu, \nu) = \sup_{f \in Lip_1(X, \mathbf{R})} \left[\int_X f(x) d\mu - \int_X f(x) d\nu \right], \tag{16}$$

where

$$Lip_1(X, \mathbf{R}) = \{f : X \to \mathbf{R} \mid |f(x_1) - f(x_2)| \leq d(x_1, x_2), \ \forall x_1, x_2 \in X\}. \tag{17}$$

For $i \leq i \leq N$, let $0 < p_i < 1$ be a partition of unity associated with the IFS maps w_i, so that $\sum_{i=1}^{N} p_i = 1$. Associated with the IFS with probabilities (IFSP) $(\mathbf{w}, \mathbf{p})$ is the so-called *Markov operator*, $M : \mathcal{M}(X) \to \mathcal{M}(X)$, the action of which is

$$\nu(S) = (M\mu)(S) = \sum_{i=1}^{N} p_i \mu(w_i^{-1}(S)), \quad \forall S \in \mathcal{H}(X). \tag{18}$$

(Here, $w_i^{-1}(S) = \{y \in X \mid w_i(y) \in S\}$.) Then M is a contraction mapping on $(\mathcal{M}(X), d_M)$ [11, 7, 1]. Consequently, there exists a unique measure $\bar{\mu} \in \mathcal{M}(X)$, the so-called *invariant measure* of the IFSP $(\mathbf{w}, \mathbf{p})$, such that $\bar{\mu} = M\mu$. Moreover, for any $\mu_0 \in \mathcal{M}(X)$, the sequence of measures $\mu_n \in \mathcal{M}(X)$ defined by $\mu_{n+1} = M\mu_n$ converges in d_M-metric to $\bar{\mu}$.

Examples:

1. $X = [0, 1]$, $N = 2$: $w_1(x) = \frac{1}{3}x$, $w_2(x) = \frac{1}{3}x + \frac{2}{3}$, as in Example 1 above, with $p_1 = p_2 = \frac{1}{2}$. Then $\bar{\mu}$ is the Cantor-Lebesgue measure supported on the Cantor set $C \subset [0, 1]$.
2. $X = [0, 1]$, $N = 2$: $w_1(x) = \frac{1}{2}x$, $w_2(x) = \frac{1}{2}x + \frac{1}{2}$. The attractor of this IFS is $[0, 1]$. When $p_1 = p_2 = \frac{1}{2}$, the IFSP invariant measure is Lebesgue measure on $[0, 1]$.
3. $X = [0, 1]$, $N = 2$: $w_1(x) = \frac{1}{2}x$, $w_2(x) = \frac{1}{2}x + \frac{1}{2}$, with $p_1 = 0.4$, $p_2 = 0.6$. The IFSP invariant measure is pictured in Figure 1 (histogram approximation).

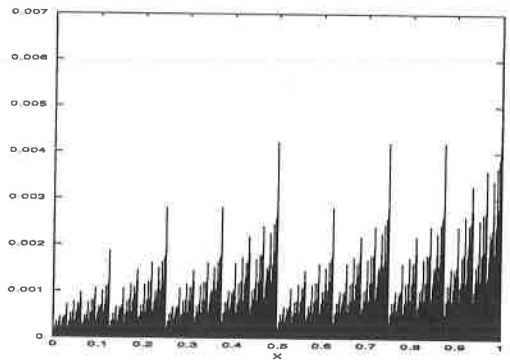

Fig. 1. Histogram approximation to the invariant measure for the IFSP in Example 3 above. (1000 bins on [0,1] were used.)

4 Continuous evolution of probability measures to fixed points of IFS Markov operators

As just mentioned, the iteration procedure,

$$\mu_{n+1} = M\mu_n, \quad n = 0, 1, 2, \cdots, \tag{19}$$

with initial condition $\mu_0 \in \mathcal{M}(X)$, produces a sequence of measures μ_i that converge in d_M-metric to the invariant measure $\bar{\mu} = M\bar{\mu}$ of the IFSP $(\mathbf{w}, \mathbf{p})$. We aim now to produce a continuous version of this evolution from μ_0 to $\bar{\mu}$. Consider measures $\mu \in \mathcal{M}(X)$ to be time-dependent, i.e., $\mu : X \times \mathbf{R} \to \mathbf{R}$. In what follows, we shall use the notations $\mu(S,t)$ and $\mu(t)$ interchangeably: the former specifically denotes the $\mu(t)$-measure of a Borel set $S \in X$.

The evolution of $\mu(S,t)$ is defined by the equation

$$\frac{\partial \mu}{\partial t} = M\mu - \mu. \tag{20}$$

This evolution equation for $\mu(S,t)$ may be interpreted as follows. Let $\mu_0 \in \mathcal{M}(X)$ be the initial value of this equation and let S be a Borel set in X. Then (20) at S is the ordinary differential equation

$$\begin{aligned} \frac{d\mu(S,t)}{dt} &= (M\mu)(S,t) - \mu(S,t) \\ &= \sum_{i=1}^{N} p_i \mu(w_i^{-1}(S), t) - \mu(S,t). \end{aligned} \tag{21}$$

Note that if $\mu_0 = \bar{\mu}$, the IFSP invariant measure, then $\mu(S,t) = \bar{\mu}(S)$ for all $t \geq 0$. It remains to show that if $\mu(0) \neq \bar{\mu}$, then $\mu(t) \to \bar{\mu}$ as $t \to \infty$ (in d_M-metric).

Eq. (21) may be integrated to yield

$$\mu(S,t) = \mu_0(S)e^{-t} + \sum_{i=1}^{N} p_i e^{-t} \int_0^t e^s \mu(w_i^{-1}(S), s)ds. \tag{22}$$

It is clear that $\mu(S,t)$ defined in (22) is a Borel measure on X. Evaluating at $S = X$ shows that $\mu(t)(X) = \mu(0)(X) = 1$. So $\mu(t) \in \mathcal{M}(X)$. Also note that if S has no preimages, i.e. $S \cap w_i(X) = \emptyset$ for $1 \leq i \leq N$, then $(M\mu)(S) = 0$ so that $\mu(S,t) = \mu_0(S)e^{-t} \to 0$ as $t \to \infty$.

Theorem 2. *Let $\bar{\mu}$ be the invariant measure of the IFSP $(\mathbf{w}, \mathbf{p})$ with associated Markov operator M, so that $M\bar{\mu} = \bar{\mu}$. Then all solutions $\mu(t)$ of Eq. (20) approach $\bar{\mu}$ exponentially as $t \to \infty$ in the d_M-metric.*

Proof. In the special case that $\mu(0) = \bar{\mu}$, it follows that the RHS of Eq. (20) is zero. This implies that $\mu(t) = \bar{\mu}$ for all $t \geq 0$. More generally, we proceed as in Section 1. Integrating Eq. (20), we obtain

$$\mu(t) = \mu(0)e^{-t} + e^{-t} \int_0^t e^s (M\mu)(s)ds. \tag{23}$$

When $\mu(0) = \bar{\mu}$, we have $\mu(t) = \bar{\mu}$ for all t and clearly,

$$\bar{\mu} = \bar{\mu}e^{-t} + e^{-t} \int_0^t e^s (M\bar{\mu})(s)ds. \tag{24}$$

Subtracting (24) from (23), multiplying the result by a function $f \in Lip_1(X, \mathbf{R})$ and integrating both sides of the resulting equation over X, there obtains

$$\begin{aligned} \left| \int_X f d\mu(t) - \int_X f d\bar{\mu} \right| \;\leq\; & e^{-t} \left| \int_X f d\mu(0) - \int_X f d\bar{\mu} \right| \\ & + e^{-t} \int_0^t e^s \left| \int_X f d(M\mu(s)) - \int_X f d(M\bar{\mu}) \right| ds. \end{aligned} \tag{25}$$

It follows immediately that

$$d_M(\mu(t), \bar{\mu}) \;\leq\; d_M(\mu(0), \bar{\mu})e^{-t} + e^{-t} \int_0^t e^s d_M(M\mu(s), M\bar{\mu})ds. \tag{26}$$

Contractivity of M on $\mathcal{M}(X)$ implies that

$$d_M(\mu(t), \bar{\mu}) \;\leq\; d_M(\mu(0), \bar{\mu})e^{-t} + ce^{-t} \int_0^t e^s d_M(\mu(s), \mu)ds. \tag{27}$$

As in Section 2, it follows that

$$d_M(\mu(t), \bar{\mu}) \;\leq\; d_M(\mu(0), \bar{\mu})e^{(c-1)t}, \quad t > 0. \tag{28}$$

Since $c \in [0, 1)$, then necessarily $d_M(\mu(t), \bar{\mu}) \to 0$ as $t \to \infty$, once again exponentially rapidly, thus proving the theorem.

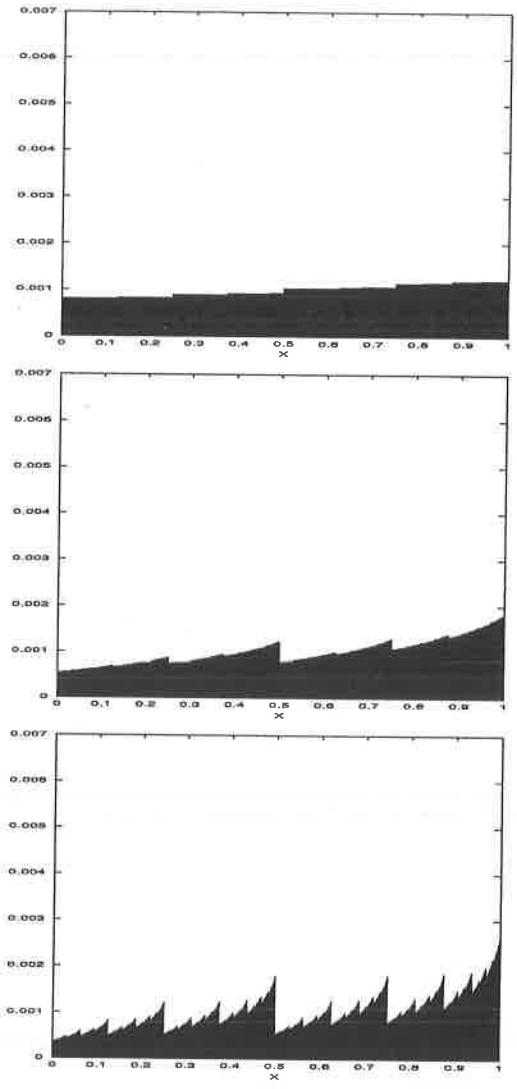

Fig. 2. Evolution of measures $\mu(t)$ toward the IFSP invariant measure of Figure 1, according to Eq. (20). Initial value is $\mu(0) = m$, Lebesgue measure on [0,1]. (a) $t = 1.0$, (b) $t = 3.0$, (c) $t = 5.0$. As in Figure 1, these are histogram approximations using 1000 bins on [0,1].

5 IFS operators on function spaces

IFS operators on function spaces $B(X)$ may be defined in a manner rather similar to that of measures [9, 10]. For the moment, we consider general function spaces $\mathcal{F}(X)$ supported on X. The essential components of a *fractal transform operator* are as follows.

1. A set of N contraction maps $w_i : X \to X$; given a function $u \in \mathcal{F}(X)$, each map w_i produces a spatially-contracted copy of u, $u_i(x) = u(w_i^{-1}(x))$ supported on the subset $X_i = w_i(X)$. **Note:** In the case of functions, we demand that $\mathbf{w}(X) = \cup_{i=1}^{N} w_i(X) = X$ so that each point $x \in X$ has at least one preimage $w_k^{-1}(x)$.
2. The $u_i(x)$ are now modified by means of *greyscale maps* $\phi_i : \mathbf{R} \to \mathbf{R}$ that satisfy suitable conditions. Usually, they are assumed to be Lipschitz so that for each ϕ_i there exists a $K_i \geq 0$ such that

$$|\phi_i(t_1) - \phi_i(t_2)| \leq K_i |t_1 - t_2|, \quad \text{for all } t_1, t_2 \in \mathbf{R}. \tag{29}$$

   The result is a set of spatially-contracted and greyscale-modified copies of u, namely, $g_i(x) = (\phi_i \circ u \circ w_i^{-1})(x)$. (The set of contraction maps w_i with associated greyscale maps ϕ_i is also referred to as an "Iterated Function System with greyscale maps" or an IFSM $(\mathbf{w}, \Phi)$ [9].)
3. These *fractal components* $g_i(x)$ are then combined – with an operation that is suitable to the space in which we are working – to produce a new function $v \in \mathcal{F}(X)$. The natural operation to combine fractal components in L^p spaces is the summation operation.

The net result of all of these operations is summarized as $v = Tu$, where $T : \mathcal{F}(X) \to \mathcal{F}(X)$ is called the *fractal transform* operator, *viz.*

$$v(x) = (Tu)(x) = \sum_{i=1}^{N} \phi_i(u(w_i^{-1}))(x). \tag{30}$$

For a given $p \geq 1$ and with suitable conditions on the IFS map contraction factors c_i and the greyscale map Lipschitz constants K_i [9], the fractal transform T is contractive on $L^p(X)$ with fixed point function $\bar{u} \in L^p(X)$. The fixed point equation,

$$\bar{u}(x) = (T\bar{u})(x) = \sum_{i=1}^{N} \phi_i(\bar{u}(w_i^{-1}))(x), \tag{31}$$

indicates that $\bar{u}$ is "self-similar," i.e., that it can be written as a sum of spatially-contracted and greyscale-modified copies of itself. Moreover, for any $u_0 \in L^p(X)$, the sequence of iterates $u_{n+1} = Tu_n$, $n = 0, 1, 2, \cdots$, converges in L^p-metric to $\bar{u}$.

The continuous evolution equation analogous to Eq. (20) is then

$$\frac{\partial u(x,t)}{\partial t} = \sum_{i=1}^{N} \phi(u(w_i^{-1}(x))) - u(x), \quad x \in X. \tag{32}$$

In most applications, the greyscale maps are assumed to have an affine form, $\phi_i(t) = \alpha_i t + \beta_i$, so that the above equation becomes

$$\frac{\partial u(x,t)}{\partial t} = \sum_{i=1}^{N} \left[\alpha_i u(w_i^{-1}(x)) + \beta I_{X_i}(x)\right] - u(x), \quad x \in X, \tag{33}$$

where $I_A(s)$ denotes the characteristic function of a set $A \in X$, i.e., $I_A(x) = 1$ if $x \in A$ and zero otherwise.

Since the fractal transform T does not contain any differential operators, Eqs. (32) and (33) are ordinary differential equations in $u(x,t)$, involving only time derivatives. Nevertheless, because of the terms $w_i^{-1}(x)$, these DE's are *nonlocal* in that the time evolution of $u(x,t)$ is determined by values of u generally *not* at x. This can lead to rather complicated evolution.

This evolution scheme and its implementation are quite similar to that discussed for measures in the previous section. As such, we do not present any examples and proceed to consider block fractal transforms in the next section.

5.1 Fractal transform operators and block image coding

It is overambitious to expect that a general image, viewed as a function or measure, would be well approximated by a union of shrunken and distorted copies of itself. Following the idea of Jacquin [12], however, it has been found that an image u may be well approximated by a union of shrunken and distorted copies of *subsets* of itself. This has been the basis of block-based fractal image coding [3, 8, 13] which is reviewed very briefly below.

For simplicity, the support X of an image will be considered as either $[0,1]^2$ (continuous support) or an $n \times n$ pixel array (discrete support). Consider a partition of X into subblocks R_i with $X = \cup_i R_i$. The R_i are assumed to be "nonoverlapping," either intersecting only at common boundaries (continuous case) or not at all (pixel case). Associated with each "range block" R_i is a larger "domain" block $D_i \subset X$ so that $R_i = w_i(D_i)$ where w_i is a 1-1 contraction map. The image function $u|_{R_i}$ supported on each R_i is also found to be well approximated by a spatially-shrunken and greyscale-modified copy of $u|_{D_i}$:

$$u|_{R_i} \approx \phi_i \circ u|_{D_i} = \phi_i \circ u|_{D_i} \circ w_i^{-1}, \quad 1 \le i \le N. \tag{34}$$

Once again, the $\phi_i : \mathbf{R} \to \mathbf{R}$ are greyscale maps that are typically affine maps in practice.

Because the range blocks are nonoverlapping, we may write the above relation as

$$u(x) \approx (Tu)(x) = \sum_i \phi_i(u(w_i(x))), \quad x \in X. \tag{35}$$

The block fractal transform operator T has the same form as the operator in Eq. (30). It is a well-known result [1] that if the "collage distance" $\| u - Tu \|$ is small, then u is well approximated by the fixed point $\bar{u}$ of T. More precisely,

$$\| u - \bar{u} \| \ \le \ \frac{1}{1-c} \| u - Tu \|, \tag{36}$$

where c is the contraction factor of the fractal transform operator T. This allows the inverse problem of fractal image coding to be reformulated into a more tractable problem. Instead of searching for a T whose fixed point $\bar{u}$ is close to u, we search for a T that maps u close to itself.

In Figure 3 is presented the fixed point approximation $\bar{u}$ to the standard 512×512 Lena image (8bpp) using a partition of 8×8 nonoverlapping pixel blocks ($64^2 = 4096$ in total). The "domain pool" for each range block was the set of $32^2 = 1024$ 16×16 non-overlapping pixel blocks. (This is clearly not optimal.) This image was obtained by starting with the seed image $u_0(x) = 255$ (plain white image) and iterating $u_{n+1} = Tu_n$ to $n = 15$. Iterates u_1, u_2 and u_3 are also shown in this figure.

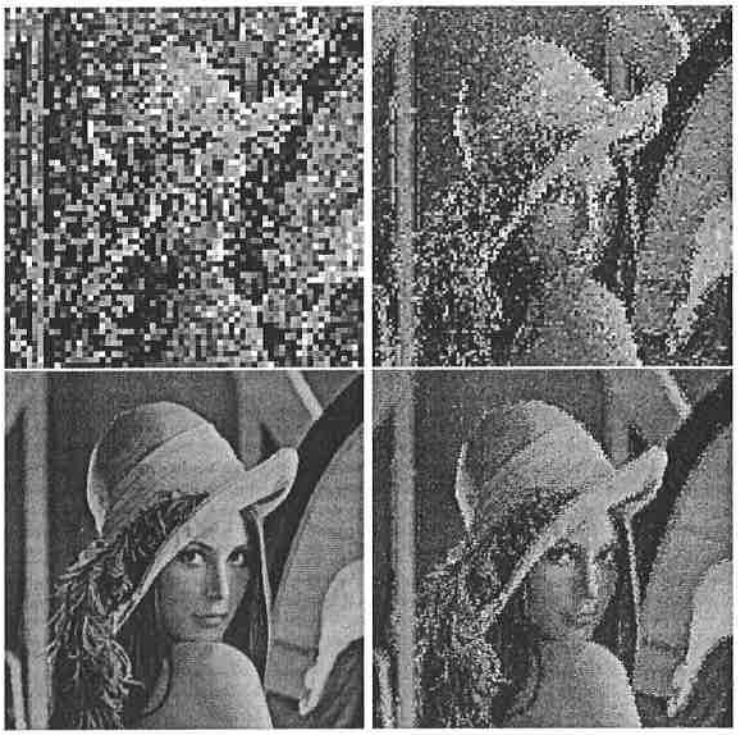

Fig. 3. Starting at upper left and moving clockwise: The iterates u_1, u_2 and u_3 along with the fixed point $\bar{u}$ of the fractal transform operator T designed to approximate the standard 512×512 (8bpp) "Lena" image. The "seed" image was $u_0(x) = 255$ (plain white). The fractal transform T was obtained by "collage coding" using 4096 8×8 nonoverlapping pixel range blocks. The domain pool consisted of the set of 1024 nonoverlapping 16×16 pixel blocks.

In Figure 4 we show the time evolution of images $u(x,t)$ as determined by $u_t = Tu - u$ where T is the fractal transform operator described above and used in Figure 3. In this case, the time evolution proceeds at a slower pace than in Figure 3, starting at $u_0 = 255$ (plain white image) and proceeding in time steps of 0.2 using a step size of $h = 0.1$ in the Euler method of Eq. (11).

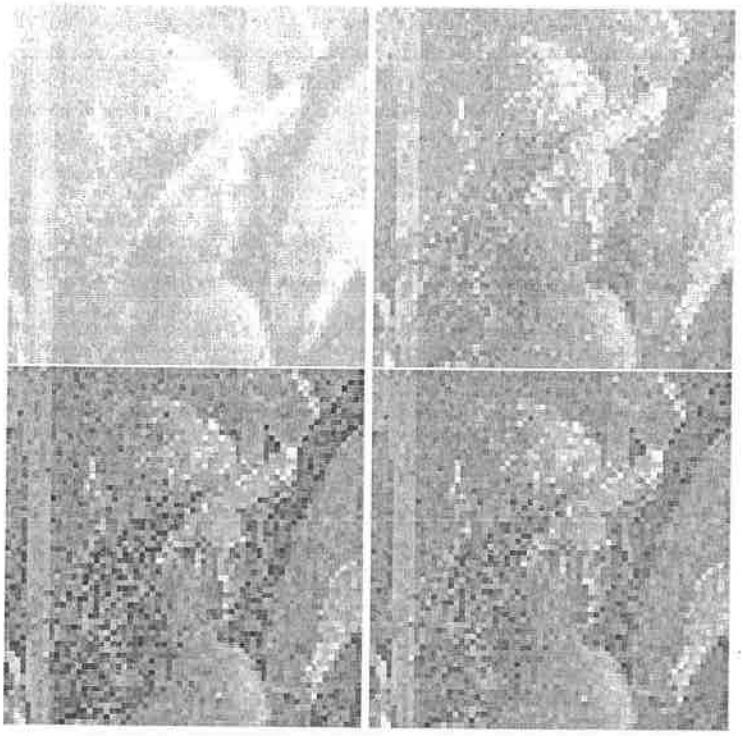

Fig. 4. Starting at upper left and moving clockwise: The images $u(x,t)$ at times 0.2, 0.4, 0.6, 0.8 produced from $u(x,0) = 255$ (plain white) under evolution by $u_t = Tu - u$ where T is the fractal transform whose discrete iteration was shown in Figure 3. Euler method, step-size $h = 0.1$.

6 Applications to complex analytic dynamics

Here we are concerned with complex iteration dynamics $z_{n+1} = R(z_n)$, where $z \in \mathbf{C}$ and $R : \mathbf{C} \to \mathbf{C}$ is a rational function of degree greater than or equal to two. The closure of the set of all repulsive k-cycles of R, $k \geq 1$, is the so-called *Julia set* J_R [4, 5].

For simplicity, the examples here will be taken from the well studied one-parameter family of quadratic maps $R(z) = z^2 + c$. When $c = 0$, the Julia set of $R(z) = z^2$ is the unit circle. The points $\bar{z} = 0$ and $\bar{z} = \infty$ are attractive fixed points of $R(z)$. The point $\bar{z} = 1$ is repulsive. The set J_R acts as a boundary between the basins of attraction of $\bar{z} = 0$ and $\bar{z} = \infty$. As c decreases from 0, the Julia set becomes "crinkly" and the finite attractive fixed point moves leftward along the negative real axis. At $c = -3/4$, this fixed point becomes neutral. Further decrease of c produces an attractive two-cycle that becomes neutral at $c = -5/4$. This is the start of the famous period-doubling bifurcation associated with this iteration

process. Much more can be written about the iteration dynamics, but we keep the discussion short here.

Following Eq. (2), the evolution equation associated with the quadratic map $R(z) = z^2 + c$ will be

$$\frac{dz}{dt} = z^2 + c - z, \tag{37}$$

where $z(t) \in \mathbf{C}$. If we let $z = x + iy$ and $c = c_1 + ic_2$, then Eq. (37) yields the system

$$\begin{aligned} \frac{dx}{dt} &= x^2 - y^2 - x + c_1, \\ \frac{dy}{dt} &= 2xy - y + c_2, \end{aligned} \tag{38}$$

of ordinary differential equations for $x(t)$ and $y(t)$. The results of the previous section do not apply globally since $R(z)$ is contractive only in neighbourhoods of its attractive fixed points. (In the quadratic case, $R(z)$ can have at most one finite attractive fixed point. Moreover, such finite attractive fixed points exist only for c values on a bounded set in $\mathbf{C}$ – the large principal cardioid region of the Mandelbrot set of $z^2 + c$.) Nevertheless, it is interesting to explore the dynamics of the system of ODEs in (38).

First consider the case $c = 0$. Using simple linearization methods, it can be shown that the point $\bar{z} = 0$ is a locally asymptotically stable equilibrium solution and that $\bar{z} = 1$ is a locally unstable equilibrium solution of (38). Numerical experiments and analysis suggest that, in contrast to the discrete case (where the basin of attraction of $\bar{z} = 0$ is the open disc $|z| < 1$), the basin of attraction of $z = 0$ is the cut plane $\mathbf{C} \setminus [1, \infty)$. All points $(a, 0)$ for $a > 1$ converge to infinity.

For $c \in \mathbf{R}$ decreasing from zero, numerical experiments show that the unique fixed point $\bar{z}_1 < 0$ continues to be the asymptotically stable equilibrium point of (38) even when it is no longer attractive for the discrete iteration process. Furthermore, the basin of attraction continues to be the cut complex plane. However, when c has a nonzero imaginary component, the cut disappears and all points, except the other finite fixed point $\bar{z}_2$, travel toward $\bar{z}_1$.

6.1 Newton's method in the complex plane

Recall that the Newton function associated with the complex valued function $f(z)$ is

$$N(z) = z - \frac{f(z)}{f'(z)}. \tag{39}$$

If $\bar{z}$ is a zero of $f(z)$, then it is also a fixed point of $N(z)$. In the discussion that follows, we assume that the zeros of $f(z)$ are simple. Then $N'(\bar{z}) = 0$, so that $\bar{z}$ is locally *superattractive*. For an initial seed $z_0 \in \mathbf{C}$ suitably close to $\bar{z}$, the iterates $z_{n+1} = N(z_n)$ converge quadratically to $\bar{z}$.

Consider the following evolution equation in the time-dependent complex variable $z(t)$ that corresponds to Eq. (2), namely,

$$\begin{aligned} \frac{dz}{dt} &= N(z) - z \\ &= -\frac{f(z)}{f'(z)}. \end{aligned} \tag{40}$$

Technically speaking, N is not necessarily a contraction mapping so that the results of Sections 2 to 5 do not apply globally. However, Eq. (40) can be integrated to give

$$f(z(t)) = f(z(0))e^{-t}. \tag{41}$$

Thus $f(z(t)) \to 0$ as $t \to \infty$. Assuming for simplicity that $f(z)$ is analytic, it follows that $z(t)$ tends to a zero of f. (There will, of course, be complications with the critical points of f.)

It is instructive to consider a couple of examples.

1. $f(z) = z^2 - 1$ with roots $\bar{z}_1 = 1$ and $\bar{z}_2 = -1$. In the classical Newton iteration method, the imaginary axis $I = N(I)$ serves as the boundary for the basins of attraction of the two roots, as originally shown by Cayley [6].
   If we let $z = x + iy$, then Eq. (40) yields the system

$$\begin{aligned} \frac{dx}{dt} &= -\frac{x}{2} + \frac{1}{2}\frac{x}{x^2+y^2}, \\ \frac{dy}{dt} &= -\frac{y}{2} - \frac{1}{2}\frac{y}{x^2+y^2}, \end{aligned} \tag{42}$$

   of ODEs in $x(t)$ and $y(t)$. As expected, the y-axis is invariant (it also contains the critical point $z = 0$) and acts as a boundary for the basins of attraction of the two roots. If $x(0) = 0$, then $x(t) = 0$ for $t > 0$. If $x(0) > 0$, then $(x(t), y(t)) \to (1, 0)$ as $t \to \infty$. If $x(0) < 0$, then $(x(t), y(t)) \to (-1, 0)$ as $t \to \infty$.
2. $f(z) = z^3 - 1$ with roots $\bar{z}_1 = 1$ and $\bar{z}_{2,3} = -\frac{1}{2} \pm i\frac{1}{2}\sqrt{3}$. Here, the boundary between the basins of attraction for the Newton iteration method is a very complicated object – the Julia set of the Newton function. From the Julia-Fatou theory of iteration of rational functions, any open neighbourhood of a point z on the Julia set must contain subsets of *each* of the basins of attraction of the roots $\bar{z}_i$. The basins of attraction of the three roots are shown in Figure 5 (left).
   Once again letting $z = x + iy$, Eq. (40) yields the following system of ODEs in $x(t)$ and $y(t)$:

$$\begin{aligned} \frac{dx}{dt} &= -\frac{x}{3} + \frac{1}{3}\frac{x^2-y^2}{(x^2+y^2)^2}, \\ \frac{dy}{dt} &= -\frac{y}{3} - \frac{2}{3}\frac{xy}{(x^2+y^2)^2}. \end{aligned} \tag{43}$$

   The Julia set boundaries are eliminated in this scheme. The basin boundaries lie on the rays $\theta = \pi/3$, $\theta = \pi$ and $\theta = -\pi/3$ as shown in Figure 5 (right). (The critical point $z = 0$ is also included in this set of boundary points.)

7 Concluding Remarks

In this paper we have introduced a method to produce a continuous evolution of a quantity y to the fixed point $\bar{y}$ of an appropriate contraction mapping T. Such a

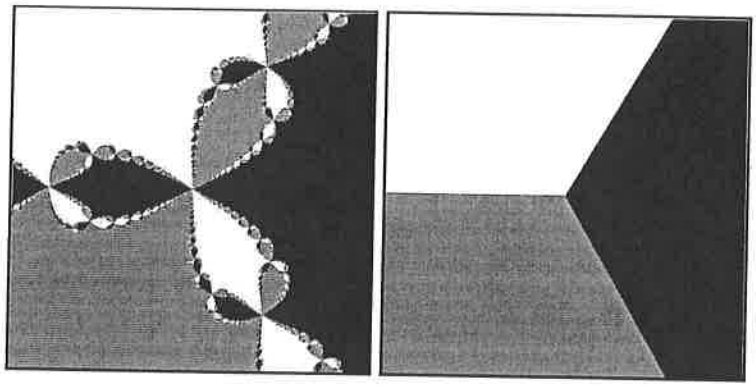

Fig. 5. Left: Basins of attraction of Newton's complex iteration method for the three cubic roots of unity. Right: Basins of attraction using the system of ODEs in Eq. (43). In both plots, the region of the complex plane being plotted is $-1 \leq Re(z) \leq 1$, $-1 \leq Im(z) \leq 1$.

continuous evolution replaces the usual discrete sequence of iterates $y_n = T^n y_0$ that converge to $\bar{y}$. The curve $y(t)$, however, does not generally interpolate the y_n. The evolution equation in Eq. (2) is not unique in that there are many possible ways of continuously "steering" the evolution of $y(t)$ to the fixed point $\bar{y}$ of the contractive operator T.

The method of Eq. (2) has been applied to two fundamental sets of contraction mappings associated with Iterated Function Systems: (1) the Markov operator M on probability measures associated to an IFS with probabilities (IFSP) and (2) the fractal transform operator T associated to IFS with greyscale maps (IFSM). We have also presented some preliminary results of applying the method to complex analytic dynamics: (1) the iteration of quadratic functions and (2) Newton's method in the complex plane.

As mentioned earlier, the original motivation to devise such a continuous evolution procedure arose from a desire to perform nonlocal, fractal-like (i.e., spatially-contracted and greyscale distorted) operations of a more continuous, i.e., "touch-up" nature. In other words, one could make arbitarily small alterations to an image function u in the neighbourhood of a point $x_0 \in X$ that would depend on values of $u(x)$ for x away from x_0.

In view of the vast research on partial differential equation methods in imaging, we envision combined fractal-based/PDE methods that could be used to produce small nonlocal alterations in the presence of diffusion-like processes. For example, one may wish to modify the evolution equation (20) by adding a small diffusion term, e.g.,

$$\frac{\partial y}{\partial t} - \epsilon \triangle y = Ty - y, \tag{44}$$

where ϵ could be either positive (diffusion) or negative (backward diffusion). Of course, such simple diffusion schemes are not generally employed in imaging. Instead, one considers "anisotropic diffusion" methods [14, 15].

Finally, the application of continuous evolution methods to complex analytic dynamics reported here is admittedly very preliminary and much remains to be explored.

Acknowledgements

We gratefully acknowledge support of this research in part by the National Science Foundation of the USA (JLB) and the Natural Sciences and Engineering Research Council of Canada (ERV).

References

1. M.F. Barnsley, *Fractals Everywhere*, Academic Press, New York (1988).
2. M.F. Barnsley and S. Demko, Iterated function systems and the global construction of fractals, *Proc. Roy. Soc. London* **A399**, 243-275 (1985).
3. M.F. Barnsley and L.P. Hurd, *Fractal Image Compression*, A.K. Peters, Wellesley, Massachusetts (1993).
4. P. Blanchard, Complex analytic dynamics on the Riemann sphere, *Bull. Amer. Math. Soc.* **11**, 85-141 (1984).
5. H. Brolin, Invariant sets under iteration of rational functions, *Ark. Math.* **6**, 103-144 (1966).
6. A. Cayley, Application of the Newton-Fourier method to an imaginary root of an equation. *Quart. J. Pure Appl. Math.* **16**, 179-185 (1879).
7. K. Falconer, *The Geometry of Fractal Sets*, Cambridge University Press, Cambridge (1985).
8. Y. Fisher, *Fractal Image Compression*, Springer Verlag, New York (1995).
9. B. Forte and E.R. Vrscay, Theory of generalized fractal transforms, in *Fractal Image Encoding and Analysis*, edited by Y. Fisher, NATO ASI Series F 159, Springer Verlag, New York (1998).
10. B. Forte and E.R. Vrscay, Inverse problem methods for generalized fractal transforms, in *Fractal Image Encoding and Analysis*, *ibid.*.
11. J. Hutchinson, Fractals and self-similarity, *Indiana Univ. J. Math.* **30**, 713-747 (1981).
12. A. Jacquin, *Image coding based on a fractal theory of iterated contractive image transformations*, *IEEE Trans. Image Proc.* **1** 18-30 (1992).
13. N. Lu, *Fractal Imaging*, Academic Press, New York (1997).
14. P. Perona and J. Malik, Scale-space and edge detection using anisotropic diffusion, *IEEE Trans. PAMI* **12**, 629-639 (1990).
15. G. Sapiro, *Geometric partial differential equations and image analysis*, Cambridge University Press, New York (2001).
16. R.F. Williams, Composition of contractions, *Bol. Soc. Brasil. Mat.* **2**, 55-59 (1971).